Available online at www.sciencedirect.com
ScienceDirect
Trans. Nonferrous Met. Soc. China 25(2015) 2003−2008
Transactions of Nonferrous Metals Society of China
www.tnmsc.cn

Uniaxial tensile behavior of porous metal fiber sintered sheet

Bo ZHOU, Wei YUAN, Jin-yi HU, Yong TANG, Long-sheng LU, Bin-hai YU

School of Mechanical and Automotive Engineering, South China University of Technology, Guangzhou 510640, China

Received 4 August 2014; accepted 12 November 2014

Abstract: A novel porous metal fiber sintered sheet (PMFSS) with a three-dimensional reticulated structure was fabricated by multi-tooth cutting and high-temperature solid-phase sintering process with copper fibers. A uniaxial tensile test was conducted to investigate the effect of fiber length and natural aging factor on the tensile properties of the PMFSS. Results indicated that, under given stress, the increase of fiber length helped reinforce the tensile strength. The elongation of the PMFSS with medium length fiber of 15 mm exhibited the optimal performance, reaching about 13.5%. After natural aging treatment for a month, the tensile strength of PMFSS significantly decreased, but the change of elongation was negligible except for the one with the shortest fiber length of 5 mm, whose elongation was effectively improved. The morphological fracture features of PMFSSs were also characterized.

Key words: porous metal fiber sintered sheet; tensile property; fiber length; natural aging; fracture mode

1 Introduction

As one of the most promising functional and structural materials, porous metal fiber sintered sheet (PMFSS) has a three-dimensional reticulated structure with interconnected pores featuring a high porosity and large specific surface area. It not only inherits the essential characteristics of the raw metal such as electrical and thermal conductivity, plasticity and machinability, but also owns special features of porous materials like layered open cell, controllable porosity and permeability, capillarity and so on [1]. Based on these superior properties, it has been widely used in various fields such as filtration and separation [2], catalytic reaction [3,4], sound absorption [5], explosion protection [6], flow field and gas diffusion [7,8], biomedical device [9], pollutant treatment [10,11], mass transfer barrier [12] and heat transfer [13,14].

To investigate the mechanical properties of PMFSS, plenty of researches were conducted in the past decades laying a good foundation for its application. ANDERSEN et al [15,16] fabricated sintered metal fiber structures using aluminum-based fibers and reported their mechanical properties. DUCHEYNE et al [17] looked into the tensile and compressive properties of novel low-porosity PMFSS made from AISI316L stainless steel fibers with diameter of 50 and 100 μm. LIU et al [18,19] made a porous steel wire mesh with open pores by using metallurgical methods and assessed the effects of forming pressure and sintering parameters on the porous structure and mechanical behavior of the wire mesh. MARKAKI et al [20] produced highly porous sheets through liquid-phase sintering of copper-coated short fibers with a diameter of 100 μm at about 1100 °C for 5 min. They found that the tensile strength of the sheets with a porosity of 90% was less than 1 MPa. QIAO et al [21] developed a PMFSS made of stainless steel fibers with a diameter of 12 μm by means of vacuum sintering. Compression testing of the porous metal fibers was carried out in a quasi-static condition. TAN and CLYNE [22] fabricated highly-porous (75%−95%) ferrous fiber network materials by use of solid-state sintering at 1200 °C for 3 h. They conducted heat treatment on single-fibers, and made micrographic characterization of the grain change. Regretfully, the effect of fiber length on tensile property was not clarified. ZHOU et al [23] focused on how the porosity and sintering parameters impacted on the tensile properties of PMFSS. JIN et al [24,25] and YI et al [26] validated a series of theoretical models disclosing the relationship between structural parameters and mechanical properties

Foundation item: Projects (51475172, 51275180, 51375177) supported by the National Natural Science Foundation of China; Project (S2013040016899) supported by the Natural Science Foundation of Guangdong Province, China; Projects (2013ZM0003, 2013ZZ017) supported by the Fundamental Research Funds for the Central Universities, South China University of Technology, China

Corresponding author: Wei YUAN; Tel: +86-20-87114634; E-mail: mewyuan@scut.edu.cn

DOI: 10.1016/S1003-6326(15)63809-2

of the PMFSS.

In view of the current literatures, the effects of fiber length parameter and natural aging factor on the tensile properties of PMFSS were barely investigated. With this background, the present work performed a uniaxial tensile test to investigate related issues regarding a self-made PMFSS. The morphological fracture features of this PMFSS were also characterized in this work.

2 Experimental

2.1 Processing procedures of PMFSS

In this experiment, the PMFSS was made of copper fibers that were prepared by multi-tooth cutting and high-temperature solid-phase sintering. The fibers were machined by a super-hard multi-tooth cutter made from W12Mo3Cr4V3N at a low speed on a horizontal lathe (C6132A), as shown in Fig. 1(a). The nominal flank face of this cutter had a row of triangle micro-teeth formed by wire-cutting. After prescribing appropriate cutter parameters and processing conditions, a string of continuous long fibers with diameters of 100−150 μm could be obtained. Detailed processing parameters can refer to our previous work [27]. The collected fibers are shown in Fig. 1(b). Subsequently, the fibers were snipped into small segments. In order to inspect the effects of fiber length, in this work, three types of fiber elements with different values of lengths were prepared, namely 5, 15 and 35 mm. Then, a specified volume of copper fibers were loaded uniformly into the packing chamber of the mold assembly in random directions. The compaction force was regulated by using M8 bolts. By altering the ratio of fiber mass to cavity volume, we could get the PMFSS samples with different porosities. Then, the fibers were sintered in a programmable furnace in the hydrogen atmosphere at a constant pressure of 0.5 MPa. The rising speed of sintering temperature was controlled at a rate of 500 °C/h, and the PMFSS was finally treated at 900 °C for 1 h. When the sintering process was completed, the PMFSS was cooled to room temperature in the furnace. Figure 2 displayed the PMFSS samples produced with different fiber lengths.

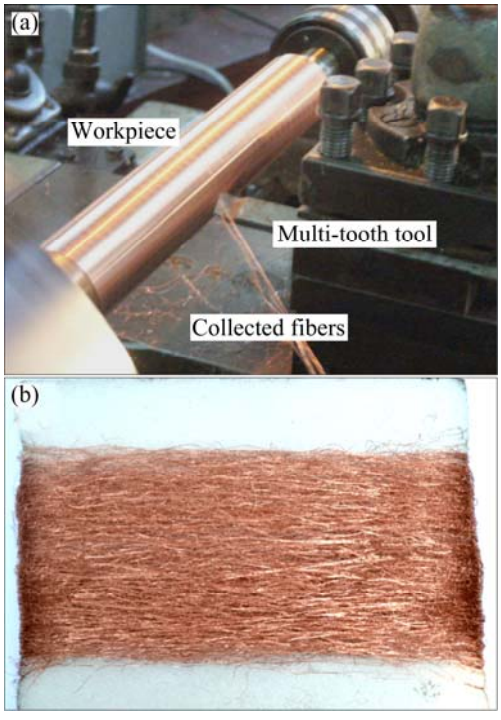

Fig. 1 In-situ photos of multi-tooth cutting process (a) and collected copper fibers (b)

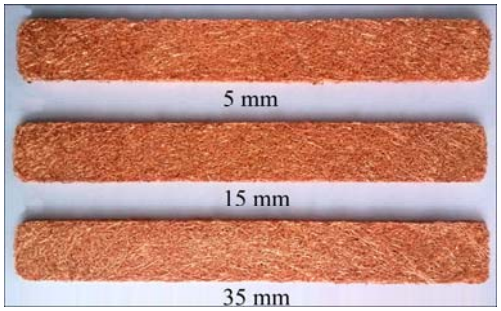

Fig. 2 PMFSS samples with different fiber lengths

Since the PMFSS has a regular geometric shape, the average porosity can be calculated by using the mass−volume method

$$E=\left(1-\frac{m}{\rho V}\right)\times 100\% \quad (1)$$

where V is the volume of PMFSS (cm^3), m is the mass of PMFSS (g) and ρ is the density of red copper (g/cm^3).

2.2 Tensile test of PMFSS

The tensile test was carried out on a universal material testing machine (INSTRON 2369, USA) with the load error less than 1% at room temperature. The cross-head speed was controlled at a constant tensile rate of 1.5 mm/min. An extensometer gauge length with 50 mm was used to measure the displacement and strain. To meet the testing requirement, the size of each PMFSS sample was 120 mm (length) × 15 mm (width) × 2 mm (thickness). The fixtures of the testing machine had a self-locking setup. For each run of test, the determinand was clamped by the fixtures by force of friction, whose effective length was actually 60 mm, as shown in Fig. 3. In this work, the elongation represents the percentage of total extension at the maximum force.

3 Results and discussion

3.1 Microstructural characterization of PMFSS with typical porous structure

Figure 4(a) shows the microscopic structure and morphology of the PMFSS with a porosity of 80%. It can

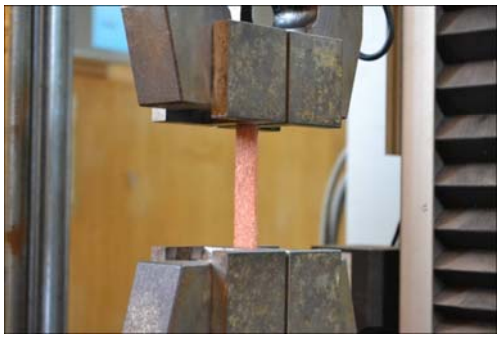

Fig. 3 Sample clamped by fixtures on universal material testing machine

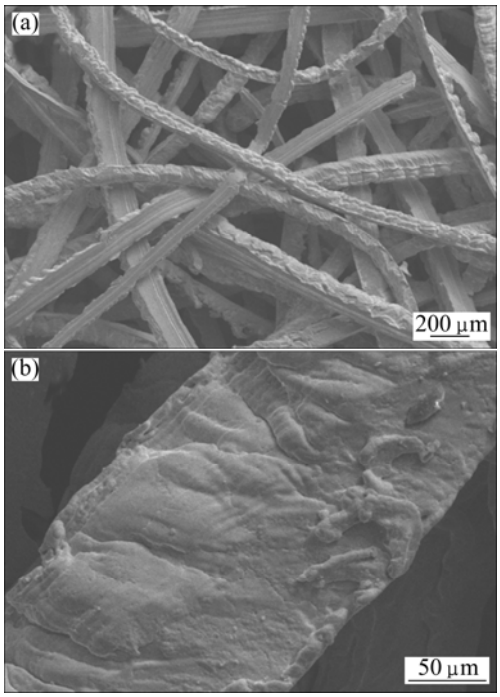

Fig. 4 SEM images of PMFSS with 80% porosity (a) and fiber surface morphology (b)

be seen that the metal fibers are randomly connected with each other to construct a metal skeleton forming a three-dimensional network structure. Apparently, many micro/nano-scale bulges grow on the surface of a single fiber, as shown in Fig. 4(b). Such a rough structure benefits forming sintering joints among the fibers, which significantly enhances the mechanical strength of the PMFSS.

3.2 Uniaxial tensile stress–strain behavior of PMFSS

The tensile stress–strain curves for the PMFSS with different fiber lengths are presented in Fig. 5. It can be found that in the initial stage, the PMFSS experiences a short period of elastic deformation. The stress–strain relationship agrees well with the linear elastic Hooke's law. As the tension increases, the fibers in the PMFSS begin to deflect plastically around the sintering joint between two fibers in the pulling direction. With a continuous increase in tensile force, the fibers and sintering joints suffer from plastic deformation. This is also a typical behavior for many other metal materials. However, no yield stage can be observed in the case of this work. This is different from the tensile property of the base material of copper. When the tension reaches the ultimate tensile stress, the fibers and sintering joints get fractured so that the stress drops sharply, leading to the destruction of the entire network structure.

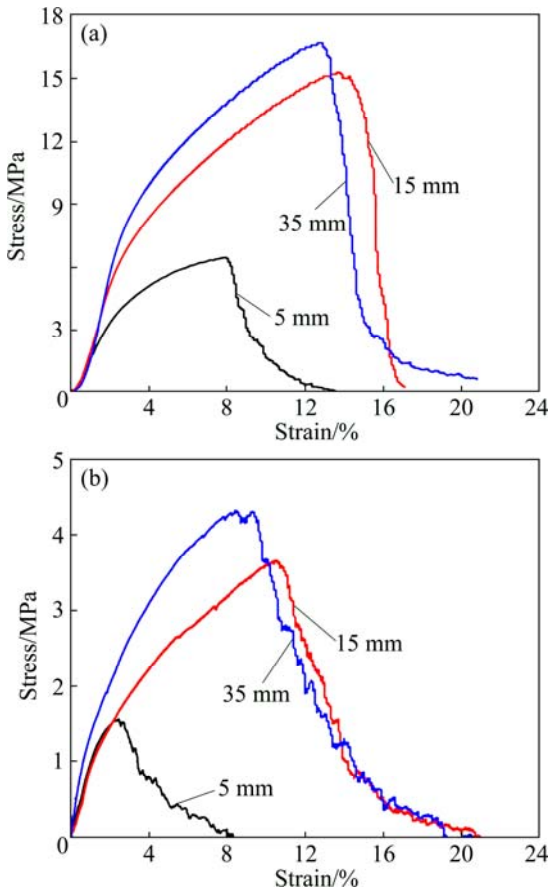

Fig. 5 Uniaxial tensile stress–strain curves for PMFSSs with different porosities: (a) 70%; (b) 80%

3.3 Effect of fiber length on uniaxial tensile fracture properties

Figure 6(a) shows the tensile strengths of PMFSS with fiber lengths of 5 mm (PMFSS-5), 15 mm (PMFSS-15) and 35 mm (PMFSS-35), respectively. In this experiment, two porosities of 70% and 80% were involved. When a porosity of 70% is used, the PMFSS-35 with the longest fiber length exhibits the optimum tensile strength at 16.7 MPa. The tensile strength of the PMFSS-15 with the medium fiber length is lower with a value of 14.5 MPa. For the PMFSS-5 based on the shortest fiber, the tensile strength drops sharply, simply reaching 6.5 MPa. Obviously, the length of fibers has a great influence on the tensile strength of

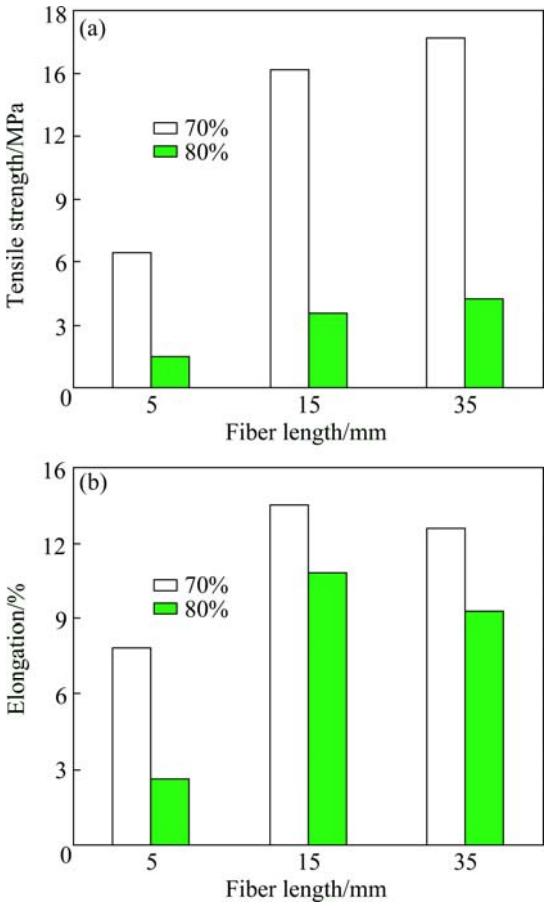

Fig. 6 Tensile properties of PMFSS: (a) tensile strength; (b) elongation

the PMFSS. As we know, throughout the sintering process, the sintering joints arise from material migration among the interlaced fibers. The size of a sintering joint is mostly small, and the stress concentration is likely to occur around the area of sintering joints. As a result, the strength of the sintering joints is much lower than that of the copper fibers. When a uniaxial load is applied, the stress transfers among the fibers and sintering joints. By comparison, the PMFSS-5 only includes short fibers with poor tensile strength to bear force, and its sintering joints are torn apart easily. Therefore, an overall fracture happens quickly. As shown in Fig. 7, the fracture occurs in a perpendicular direction to the tensile loading, showing similar behavior to brittle materials. For the medium fiber length of 15 mm, the fracture of the PMFSS-15 emerges at an angle of 45° relative to the tensile loading direction. This result is consistent with that reported by ZHOU et al [23]. Theoretically, this phenomenon follows the maximum shear stress criterion according to the plastic flow failure mode of metal materials. When the fiber length reaches 35 mm, necking phenomenon which usually happens in the tensile fracture of plastic metal materials can be observed finally, and the tensile strength gets to a higher level of about 16.7 MPa. The above results demonstrate that the use of long fibers contribute to improving the strength of the PMFSS. Likewise, the 80% PMFSSs have analogous tensile behavior but exhibit far lower tensile strength correspondingly at a given fiber length. This is owing to smaller effective bearing area and fewer sintering joints associated with larger porosities. It can be thus far confirmed that the tensile strength of the PMFSS is quite sensitive to its porosity.

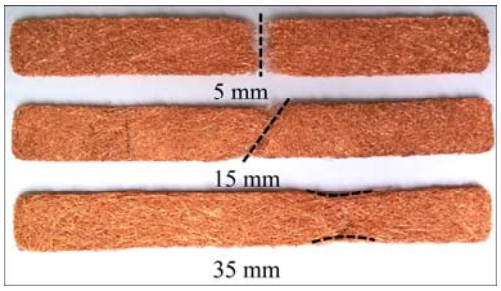

Fig. 7 Fractured morphology of PMFSS samples with different fiber lengths

As shown in Fig. 6(b), no matter which porosity is adopted, the elongation of the PMFSS-15 is the highest, followed by PMFSS-35 and PMFSS-5 because the former achieves a good balance between fiber length and fiber joints. On one hand, the use of a medium fiber length, i.e., 15 mm, provides enough resistance to the change of tension. On the other hand, the effective formation of fiber joints enhances stress transfer and promotes uniaxial extension by plastic deformation around fiber joints. This rule is of great importance to material design, suggesting how to choose the fiber length according to the requirements of material mechanical property related to tensile strength and elongation.

After being treated by natural aging and placed in a confined space at a room temperature of 26 °C for 1 month, the PMFSS shows diverse tensile behaviors, as shown in Fig. 8(a). Interestingly, after the sample experiences a short period of elastic deformation process, obvious yield stages can be observed for all PMFSSs with different fiber lengths when the tensile stress is around 1.3 MPa, as shown in Fig. 8(b). This hints that the samples tested in this situation have a similar performance to the plastic metal material. Compared with Figs. 5 and 6, it is found that the tensile strength of PMFSS is significantly reduced. This may be ascribed to the effect of grain growth of fibers and sintering joints after the natural aging treatment. Nevertheless, the stress concentrating around the sintering joints is more likely to release with the test going on. As a result, the elongations of the PMFSS-15 and PMFSS-35 almost remain, whereas the PMFSS-5 gains an improved elongation because it is much more sensitive to stress

concentration around the sintering joints. Therefore, it is better to take the time-related factor into account for material design and application.

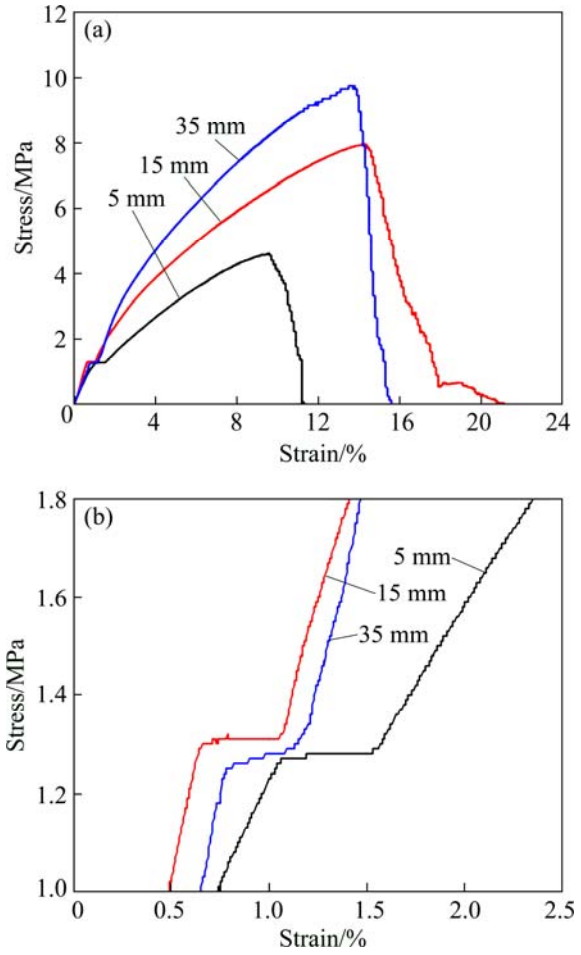

Fig. 8 Uniaxial tensile stress−strain curves for PMFSSs after 1 month (a) and magnification of yield stages (70% porosity) (b)

4 Conclusions

1) The fiber length has a significant effect on the fracture mode of the PMFSS. The PMFSS-5 made of 5 mm fibers is destroyed in the form of brittle fracture. The PMFSS-15 with a medium fiber length of 15 mm fractures at an angle of 45° relative to the tensile loading direction. The PMFSS-35 with 35 mm fibers is damaged along with necking phenomenon.

2) The tensile strength of a PMFSS increases with the increase in fiber length. The PMFSS constructed by medium-length fibers owns the highest elongation. To balance the tensile strength and elongation, the PMFSS with a medium fiber length is recommended for material design.

3) The effect of natural aging leads to an obvious yield stage during the tensile process. As a result, the tensile strength of the treated samples significantly decreases, but the elongation almost remains except for the PMFSS-5 whose elongation is effectively improved.

References

[1] YUAN Wei, TANG Yong, YANG Xiao-jun, WAN Zhen-ping. Porous metal materials for polymer electrolyte membrane fuel cells—A review [J]. Applied Energy, 2012, 94: 309−329.

[2] AYDIN N, EDWARD W L, ANTONIO C M S. A general model for the permeability of fibrous porous media based on fluid flow simulations using the lattice Boltzmann method [J]. Composites: Part A, 2009, 40: 860−869.

[3] YURANOV I, KIWI-MINSKER L, RENKEN A. Structured combustion catalysts based on sintered metal fibre filters [J]. Applied Catalysis B: Environmental, 2003, 43: 217−227.

[4] YURANOV I, RENKEN A, KIWI-MINSKER L. Zeolite/sintered metal fibers composites as effective structured catalysts [J]. Applied Catalysis A: General, 2005, 281: 55−60.

[5] ZHANG Bo, CHEN Tian-ning. Calculation of sound absorption characteristics of porous sintered fiber metal [J]. Applied Acoustics, 2009, 70: 337−346.

[6] MARKUS D, MECKE S, FORSTER H. Endurance burning flame arresters using sintered metal fibres [J]. Forsch Ingenieurwes, 2009, 73: 17−23.

[7] KUO J K, CHEN C K. A novel Nylon-6-S316L fiber compound material for injection molded PEM fuel cell bipolar plates [J]. Journal of Power Sources, 2006, 162: 207−214.

[8] ANDERSEN O, MEINERT J. Heat Transfer and fluid flow in sintered metallic fiber structures [J]. Material Science Forum, 2010, 638−642: 1884−1889.

[9] RYAN G E, PANDIT A S, APATSIDIS D P. Porous titanium scaffolds fabricated using a rapid prototyping and powder metallurgy technique [J]. Biomaterials, 2008, 29: 3625−3635.

[10] YE Zhi-ping, WANG Chun-xia, SHAO Zhen-hua, YE Qing, HE Yi, SHI Yao. A novel dielectric barrier discharge reactor with photocatalytic electrode based on sintered metal fibers for abatement of xylene [J]. Journal of Hazardous Materials, 2012; 241−242: 216−223.

[11] NIKOLAJSEN K, KIWI-MINSKER L, RENKEN A. Structured fixed-bed adsorber based on zeolite/sintered metal fibre for low concentration VOC removal [J]. Chemical Engineering Research and Design A, 2006, 84(7): 562−568.

[12] YUAN Wei, TANG Yong, YANG Xiao-jun, LIU Bin, WAN Zhen-ping. Manufacture, characterization and application of porous metal-fiber sintered felt used as mass-transfer-controlling medium for direct methanol fuel cells [J]. Transactions of Nonferrous Metals Society of China, 2013, 23(7): 2085−2093.

[13] ABDULJALIL A S, YU Zhi-bin, JAWORSKI A S. Selection and experimental evaluation of low-cost porous materials for regenerator applications in thermoacoustic engines [J]. Materials and Design, 2011, 32: 217−228.

[14] VEYHL C, FIEDLER T, ANDERSEN O, MEINERT J, BERNTHALER T, BELOVA I V, MURCH G E. On the thermal conductivity of sintered metallic fibre structures [J]. International Journal of Heat and Mass Transfer, 2012, 55: 2440−2448.

[15] ANDERSEN O, STUDNITZKY T, KOSTMAN C, STEPHANI G. Sintered metal fiber structures from aluminium based fibres-manufacturing and properties [C]//Proceedings of the Fifth International Conference on Porous Metals and Metallic Foams—MetFoam. Lancaster, Montreal, Canada, 2008: 509−512.

[16] VEYHL C, FIEDLER T, JEHRING U, ANDERSEN O, BERNTHALER T, BELOVA I V, MURCH G E. On the mechanical properties of sintered metallic fibre structures [J]. Materials Science and Engineering A, 2013, 562: 83−88.
[17] DUCHEYNE P, AERNOUDT E, MEESTER P. The mechanical behaviour of porous austenitic stainless steel fibre structures [J]. Journal of Materials Science, 1978, 13: 2650−2658.
[18] LIU P, HE G, WU L H. Fabrication of sintered steel wire mesh and its compressive properties [J]. Materials Science and Engineering A, 2008, 489: 21−28.
[19] LIU P, HE G, WU L H. Uniaxial tensile stress–strain behavior of entangled steel wire material [J]. Materials Science and Engineering A, 2009, 509: 69−75.
[20] MARKAKI A E, GERGELY V, COCKBURN A, CLYNE T W. Production of a highly porous material by liquid phase sintering of short ferritic stainless steel fibres and a preliminary study of its mechanical behavior [J]. Composites Science and Technology, 2003, 63: 2345−2351.
[21] QIAO Ji-chao, XI Zheng-ping, TANG Hui-ping, WANG Jian-yong, ZHU Ji-lei. Compressive behavior of porous metal fibers [J]. Rare Metal Materials and Engineering, 2008, 37: 2173−2176.
[22] TAN J C, CLYNE T W. Ferrous fiber network materials for jet noise reduction in aeroengines Part II: Thermo-mechanical Stability [J]. Advanced Engineering Materials, 2008, 10(3): 192−200.
[23] ZHOU Wei, TANG Yong, PAN Min-qiang, WEI Xiao-ling, XIANG Jian-hua. Experimental investigation on uniaxial tensile properties of high-porosity metal fiber sintered sheet [J]. Materials Science and Engineering A, 2009, 525: 133−137.
[24] JIN M Z, CHEN C Q, LU T J. The mechanical behavior of porous metal fiber sintered sheets [J]. Journal of the Mechanics and Physics of Solids, 2013, 61: 161−174.
[25] ZHAO T F, JIN M Z, CHEN C Q. A phenomenological elastoplastic model for porous metal fiber sintered sheets [J]. Materials Science and Engineering A, 2013, 582: 188−193.
[26] YI Pei-yun, PENG Lin-fa, LIU Ning, LAI Xin-min, NI Jun. A micromechanics elastic–plastic constitutive model for sintered stainless steel fiber felt [J]. Materials and Design, 2013, 51: 876−885.
[27] YUAN Wei, TANG Yong, YANG Xiao-jun, LIU Bin, WAN Zhen-ping. On the processing and morphological aspects of metal fibers based on low-speed multi-tooth dry cutting [J]. International Journal of Advanced Manufacturing Technology, 2013, 66(5−8): 1147−1157.

多孔金属纤维烧结毡单向拉伸行为

周 波，袁 伟，胡进溢，汤 勇，陆龙生，余彬海

华南理工大学 机械与汽车工程学院，广州 510640

摘 要：基于多齿刀具切削及高温固相烧结铜纤维技术制备具有三维网状结构的多孔金属纤维烧结毡(PMFSS)。通过单向拉伸试验研究纤维长度及自然时效处理对 PMFSS 拉伸性能的影响。结果表明：增大纤维长度有利于提高 PMFSS 的拉伸强度；选用 15 mm 中等纤维长度有利于 PMFSS 获得最优的伸长率，可达到 13.5%。经 1 个月的自然时效处理后，PMFSS 的拉伸强度都出现明显下降，但除 5 mm 短纤维 PMFSS 的伸长率明显提高，其他 PMFSS 伸长率基本保持不变。同时，还对 PMFSS 的断裂形式进行表征与分析。

关键词：多孔金属纤维烧结毡；拉伸性能；纤维长度；自然时效；断裂形式

(Edited by Yun-bin HE)